

6-6-2011

An All Graphene Low Noise Amplifier

Saptarshi Das

Doctoral Student, sdas@purdue.edu

Joerg Appenzeller

Birck Nanotechnology Center, Purdue University

Follow this and additional works at: <http://docs.lib.purdue.edu/nanopub>

 Part of the [Electrical and Electronics Commons](#), [Electronic Devices and Semiconductor Manufacturing Commons](#), [Nanoscience and Nanotechnology Commons](#), and the [VLSI and Circuits, Embedded and Hardware Systems Commons](#)

Das, Saptarshi and Appenzeller, Joerg, "An All Graphene Low Noise Amplifier" (2011). *Birck and NCN Publications*. Paper 779.
<http://dx.doi.org/10.1109/RFIC.2011.5940628>

This document has been made available through Purdue e-Pubs, a service of the Purdue University Libraries. Please contact epubs@purdue.edu for additional information.

An All-Graphene Radio Frequency Low Noise Amplifier

Saptarshi Das and Joerg Appenzeller, Fellow, IEEE

Department of Electrical and Computer Engineering, Purdue University, West Lafayette, IN, USA

ABSTRACT — In this paper, we propose and quantitatively evaluate an “All-Graphene nano-ribbon (GNR) circuit” for high frequency low noise amplifier (LNA) applications, which shows considerable advantage over state-of-the-art technologies. In particular, we discuss how to satisfy the requirements for temperature stability, gain, power dissipation, noise and speed for a high performance LNA circuit by adjusting only the width of the nano ribbons. Our calculations predict a nano-ribbon width in the range of 8-12 nm to be ideal for these types of applications – different from logic applications that are expected to require much smaller ribbon widths.

Index Terms — graphene, RF, LNA, nano-ribbon,

I. INTRODUCTION

Since its discovery, graphene ⁽¹⁾, a single layer of graphite, has received significant scientific interest due to its remarkable electrical, chemical, mechanical and optical properties. Graphene being a gapless semiconductor is not the ideal choice for logic applications, but the high carrier mobility coupled with ballistic transport makes graphene field-effect transistors (GFETs) ^(2,3,4,5) a potential candidate for improving state-of-the-art analog technologies.

The basic building blocks of an LNA ⁽⁶⁾ circuit are a transistor amplifier and a load resistance, as shown in figure (1a). In this paper we discuss the implementation of the same circuit employing an “All-Graphene” approach as shown in figure (1b) and discuss how to use the width of the graphene nano ribbon as the only design parameter (figure 1c & 1d). Our analysis includes the detailed impact of the width of the graphene nano-ribbon on the voltage gain (G), speed or bandwidth (f_T), power dissipation (P), noise power (N_s) and temperature stability (S) of an RF circuit. We find that a width in the range of 8-12 nm allows for optimum performance.

II. RF LNA PARAMETERS

In this paper we will focus on low input power LNA’s (maximum signal strength 100 μ V as found in e.g. satellite and long distance radio communications) where the most important parameters are gain (G) bandwidth (f_T), power dissipation (P), noise (N_s) and temperature used conventional equations for RF circuit parameters as defined in equation (1). g_m , g_d , R_L are the small signal

transconductance, output conductance and load resistance

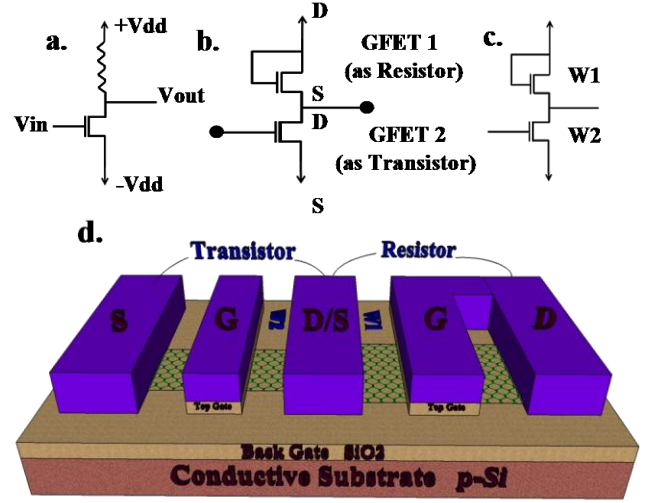


Figure 1. a) A generic LNA circuit. b) All-Graphene LNA circuit c) Width design for the All-Graphene LNA circuit. d) Layout for All-Graphene LNA circuit

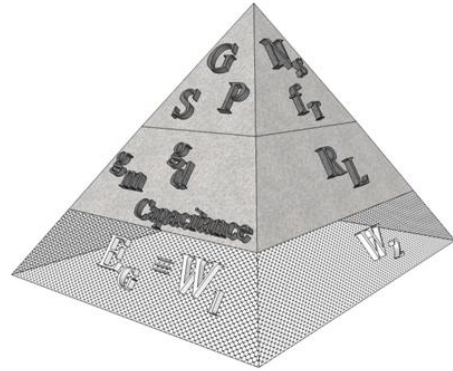


Figure 2. Top-down pyramidal view of RF-relevant variables.

$$G = \frac{g_m}{\frac{1}{R_L} + g_d} \quad f_T = \frac{g_m}{2\pi C_{in}} \quad P = V_{ds} I_{ds} + I_{ds}^2 R_L$$

$$N_s = 2qI_{op} f_T \quad S = 1 - F \quad F = \frac{1}{G} \frac{dG}{dT} \Delta T \quad (1)$$

stability (S). We have used conventional equations for RF circuit parameters as defined in equation (1). g_m , g_d , R_L are the small signal transconductance, output conductance and load resistance of the GNRFET respectively. C_{in} is the total input capacitance including parasitic contributions due to the overlap between the gate and the source/drain contacts. In particular, C_{in} is assumed to be proportional to the channel width W which holds true if the interconnect capacitances are not the dominant part. I_{ds} and V_{ds} are the operating current and voltage for the GFET. T is the temperature and S and F denote temperature stability and temperature fluctuation respectively. ΔT is the operating temperature range for the RF device. E_G is the bandgap created in the graphene nano-ribbon due to size quantization. It has been experimentally demonstrated that the bandgap of graphene nano-ribbons is inversely proportional to the width of the ribbon ⁽⁷⁾ and the empirical relationship found is given by equation (2), where “ k ” is a constant. For numerical purposes, we will use $k = 0.8$ ⁽⁷⁾.

$$E_g = \frac{k}{W \text{ in nm}} eV \quad (2)$$

It is evident from the top down pyramidal structure that the desired conditions to enable high performance RF LNAs can be obtained by tuning the width of the nano-ribbons. The challenge is therefore to find the widths that optimize the above defined performance matrix.

III SIMULATION

Graphene is a two-dimensional hexagonal lattice exhibiting a linear energy dispersion relationship. In order to model the current transport through a graphene nano-ribbon FET we have used the Landauer Formalism ⁽⁸⁾ assuming ballistic transport conditions and ignoring contact effects that would impact the total transmission probability from source to drain.

$$I = q \int_0^{\max(qV_{ch}, qV_{ds})} D(E)v(E) (f_s - f_d) dE \quad (3)$$

In this expression $v(E)$ is the carrier velocity, f_s and f_d are the source and drain Fermi functions respectively, V_{ch} is the channel potential and V_{ds} is the source-to-drain potential. In our model we have also included the tunneling current across the bandgap from source to drain. The device is assumed to be operating in the quantum capacitance limit (QCL), which results in a one-to-one band control of the channel potential (V_{ch}) with the gate bias (V_{gs}) even in the on-state of the device. The transfer and output characteristics of a GNRFET are shown in figure 3.

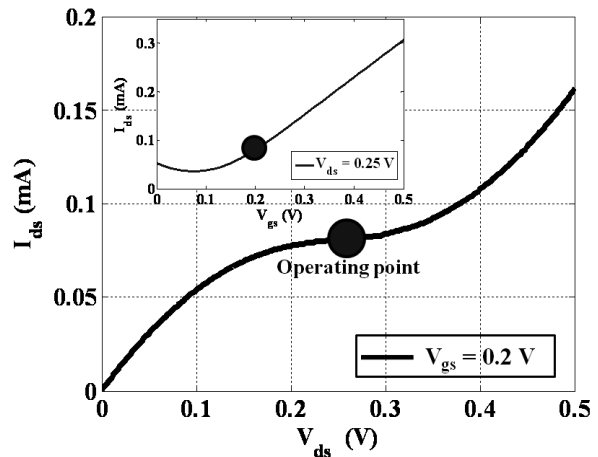


Figure 3. Output and transfer (inset) characteristics of a 10 nm wide GNRFET at room-temperature.

IV. g_m , g_d AND WIDTH (BANDGAP)

In an earlier article ⁽⁹⁾ we have identified that the transconductance and output conductance depends strongly on the dc bias point of the GNRFET of a given width and the optimum operating point for a device in the QCL is given by equation (4).

$$V_{ds} = V_{ch} + \frac{E_g}{2}, V_{gs} = V_{ch} \quad (4)$$

In order to evaluate the impact of width (bandgap) on g_m and g_d we will assume that the GNRFET is biased at the optimum operating point, with $V_{ch}=0.2V$ in the quantum capacitance limit for the remainder of the discussion. The transconductance g_m is directly proportional to the number of modes contributing to conduction and since the current flow is uniform across the width, the number of these conducting modes is directly proportional to the width (W) of the graphene nano-ribbon. Since W is proportional to $1/E_g$ according to equation (1), one finds that:

$$g_m \propto W \propto \frac{1}{E_g} \quad (5)$$

The only way to obtain current saturation in a ballistic FET is through a sizable bandgap. The voltage span of this flat saturation region is exactly equal to the bandgap, smeared out by the broadening of the Fermi function at finite temperatures. This broadening is of the order of a few $k_B T/q$ (k_B is Boltzmann constant). The output

conductance g_d , which is the slope of the $I_d - V_{ds}$ curve, of such a device in the saturation region, is close to zero. But for not too aggressively scaled GNR-FETs, the bandgap is of the order of $k_B T$ at room temperature and hence g_d is finite and shows a strong temperature and bandgap dependence. The empirical relationship between temperature, bandgap and g_d is found by simulation and is given by equation (6).

$$g_d = \frac{\chi(T)}{E_g^{1.5+0.001(T-300)}} \quad (6)$$

Equation (6) is a fit with $\chi(T)$ being a very weakly temperature dependent function which is almost constant for the temperature range considered here.

V. RF PARAMETER MATRIX AND WIDTH (BANDGAP)

The bandwidth f_T , being proportional to the ratio of g_m and C_{in} , is independent of width (bandgap), because both g_m and C_{in} are directly proportional to the width. Therefore the shot noise power N_s , which is directly proportional to the product of operating current and bandwidth, is also independent of bandgap. For a 100nm long ballistic GNR-FET, f_T -values in the THz range can be expected even with moderate parasitic capacitance contribution of $100\text{fF}/\mu\text{m}^2$.

LNAs, operating under temperature conditions ranging from -100°C to $+200^\circ\text{C}$, require adequate temperature stability. Since the bandgap of GNR-FETs is at best of the order of $k_B T$ at room-temperature, T has a significant impact on g_d as evident from equation (6). However g_m and C_{in} are almost independent of temperature. Thus it is clear that f_T remains unaffected by temperature while the voltage gain is highly sensitive to temperature variations. We define temperature fluctuations F as in equation (7). Figure 4 shows how the stability S which is defined as $1-F$, changes as a function of bandgap for different load resistances. It is evident that a larger bandgap improves stability, but the same stability value can also be achieved when using a smaller bandgap in combination with a smaller load resistance.

$$F = \frac{1}{G} \frac{dG}{dT} \Delta T = \frac{R_L}{1 + R_L g_d} \frac{dg_d}{dT} \Delta T$$

$$= R_L \frac{g_d(T_{500K}) - g_d(T_{250K})}{R_L g_d(T_{300K}) + 1} \quad (7)$$

At the optimum operating point, when the load resistance is much smaller than the output resistance, the

gain G takes the form of equation (8). The inset of figure 4 shows how the gain G changes as a function of bandgap for different load resistances. It is obvious that a smaller bandgap improves gain, but the same gain can also be achieved when using a larger bandgap in combination with a larger load resistance. Table 1 summarizes the findings of this section.

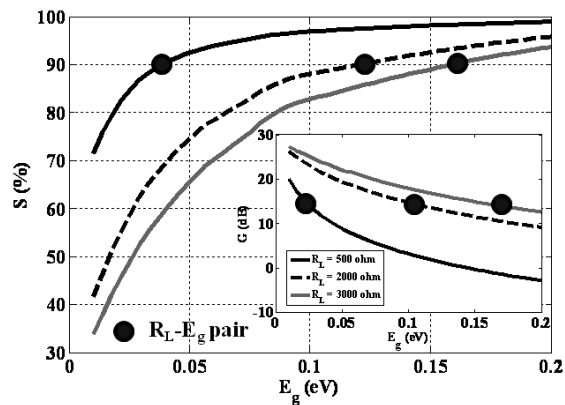


Figure 4. Stability and gain (inset) as a function of bandgap for different load resistance values R_L .

$$G = \frac{R_L g_m}{R_L g_d + 1} = \frac{R_L \gamma}{E_g} \quad (8)$$

SUMMARY TABLE I

	E_g	R_L
Bandwidth	No Dependence	No Dependence
Noise figure	No Dependence	No Dependence
High Gain	Small	Large
High Stability	Large	Small

VI. OPTIMIZATION

From figure 4 we conclude that a fixed value of S or G are obtained for a particular set of (R_L, E_g) -values. These (R_L, E_g) pairs can be used to construct a constant stability and constant gain contour line as shown in figure 5. Constant power dissipation (P) contours are vertical straight line with no bandgap dependence as evident from equation (9). Any (R_L, E_g) pair lying above the constant stability contour, below the constant gain contour, and on the left side of the constant power contour satisfies the demands in terms of S , G and P . In figure 5 we have used

$G=15\text{dB}$, $S=90\%$ and $P=50\mu\text{W}$ per device and the dots represents the (R_L, E_g) pairs satisfying these particular requirements. For different values of S , G , P as demanded by the type of application under consideration one obtains

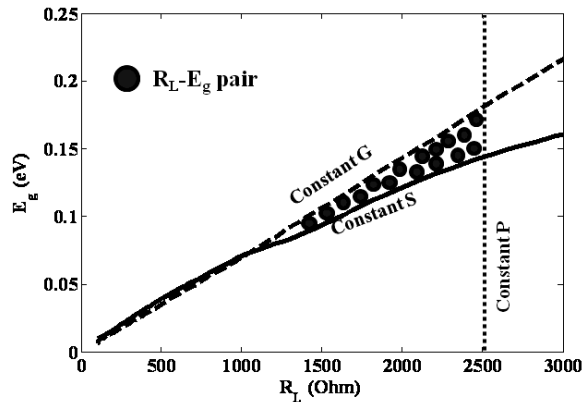


Figure 5. Constant stability, constant gain and constant power dissipation contours.

different pairs.

$$P = V_{op} I_{op} + R_L I_{op}^2 \quad (9)$$

VII. DESIGN SCHEME

Once a particular pair of (R_L, E_g) -values has been selected, the next step for a circuit engineer is to identify the associated widths of the graphene nano-ribbons (W_1, W_2) for the corresponding circuit elements, namely the load resistor and the transistor amplifier. A GNR-FET with the source and gate terminal being shorted acts as a voltage dependent resistor whose resistance value is determined by the number of conducting modes and hence the width of the nano-ribbon (W_1). Figure 6a) shows the dependence of R_L on W_1 for a given bias voltage (V_{bias}). The bias voltage is the product of R_L and I_{ds} and the supply voltage (V_{DD}) is given by equation (10).

$$V_{DD} = \frac{(V_{ds} + V_{bias})}{2} \quad (10)$$

The $E_g - W_2$ dependence mentioned in equation (2) is depicted in figure (6b). Using figure 5 and 6, designers can easily map (R_L, E_g) pairs onto the respective (W_1, W_2) pairs.

VIII. CONCLUSION

In summary, to design an All-Graphene LNA circuit, one first has to find the optimum values of load resistance and bandgap (R_L, E_g) in order to meet the

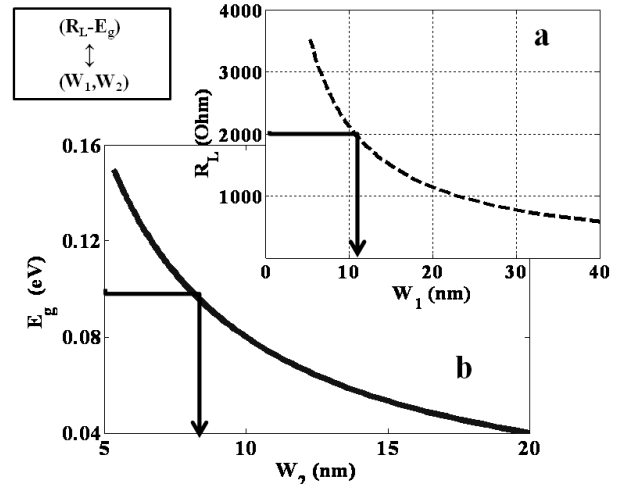


Figure 6. a) Load resistance as a function of graphene nano-ribbon width at a fixed V_{bias} b) bandgap as a function of nano-ribbon width.

requirement for a given gain, stability and power dissipation matrix (G, S, P). Then the desired (R_L, E_g) values can be adjusted by the proper choice of nano-ribbon width. For an LNA application that requires a minimum gain of 15dB and stability of 90% with power dissipation per device of less than $50\mu\text{W}$, our findings indicate that an all graphene LNA circuit can be implemented using graphene nano-ribbons of width in the range of 8-15 nm.

ACKNOWLEDGEMENT

This work was supported by the Nanotechnology Research Initiative (NRI) through a supplemental grant to the Network for Computational Nanotechnology (NCN), which is supported by the National Science Foundation (NSF) under grant number: EEC-0634750.

REFERENCES

- [1]. Geim, A. K. et al., Nature Materials, vol. 6, page 183–191 (2007)
- [2]. P.R.Wallace et al., Physical Review, vol. 71, page 622-634 (1947)
- [3]. Sandip Niyogi et al., J. Am. Chem. Soc, vol. 128 (24), page 7720–7721 (2006)
- [4]. C. Lee et al., Science, vol.321 (5887), page 385-388 (2008)
- [5]. Y.Zhang et al., Nature, vol.459 (7248), page 820–823 (2009)
- [6]. Hakan Kuntman et al., Analog Integrated Circuit Signal Process, vol. 60, page 169–193 (2009)
- [7]. P.Kim et al., Physical Review Letter, vol. 98, page 206805 (2007)
- [8]. Landauer et al., IBM J. Res Dev, vol 32, page 306 (1988).
- [9]. Saptarshi et al., IEEE TNANO, accepted for publication (2011).